Proc. Natl. Acad. Sci. USA
Vol. 95, pp. 7127–7132, June 1998
Neurobiology

Acoustic overstimulation increases outer hair cell Ca^{2+} concentrations and causes dynamic contractions of the hearing organ

(noise-induced hearing loss/guinea pig/micromechanics/image analysis/cochlear microphonic potential)

ANDERS FRIDBERGER*†, ÅKE FLOCK*, MATS ULFENDAHL‡, AND BRITTA FLOCK*

*Department of Physiology and Pharmacology, Karolinska Institutet, S-171 77 Stockholm, Sweden; and ‡King Gustaf V Research Institute, Karolinska Hospital, S-171 76 Stockholm, Sweden

Communicated by Jozef J. Zwislocki, Syracuse University, Syracuse, NY, March 31, 1998 (received for review October 27, 1997)

ABSTRACT **The dynamic responses of the hearing organ to acoustic overstimulation were investigated using the guinea pig isolated temporal bone preparation. The organ was loaded with the fluorescent Ca^{2+} indicator Fluo-3, and the cochlear electric responses to low-level tones were recorded through a microelectrode in the scala media. After overstimulation, the amplitude of the cochlear potentials decreased significantly. In some cases, rapid recovery was seen with the potentials returning to their initial amplitude. In 12 of 14 cases in which overstimulation gave a decrease in the cochlear responses, significant elevations of the cytoplasmic $[Ca^{2+}]$ in the outer hair cells were seen. $[Ca^{2+}]$ increases appeared immediately after terminating the overstimulation, with partial recovery taking place in the ensuing 30 min in some preparations. Such $[Ca^{2+}]$ changes were not seen in preparations that were stimulated at levels that did not cause an amplitude change in the cochlear potentials. The overstimulation also gave rise to a contraction, evident as a decrease of the width of the organ of Corti. The average contraction in 10 preparations was 9 μm (SE 2 μm). Partial or complete recovery was seen within 30–45 min after the overstimulation. The $[Ca^{2+}]$ changes and the contraction are likely to produce major functional alterations and consequently are suggested to be a factor contributing strongly to the loss of function seen after exposure to loud sounds.**

Noise-induced hearing loss is a common condition that leads to considerable communication problems for affected individuals. Recent research on the physiology of this condition (reviewed in ref. 1) has been mainly focused on damage to the stereocilia (SC) of the sensory cells in the inner ear, important because this is the location of the ion channels converting mechanic vibrations into electric currents. Damage to the SC correlates well with alterations of the tuning curves of auditory nerve fibres (2). A capacity for repair of the SC after acoustic trauma also has been implicated (3), but the mechanisms underlying the stereociliary changes as well as the repair process remain unknown.

Acoustic trauma also may cause degeneration of the sensory cells, resulting in an irreversible elevation in hearing thresholds (4). The degeneration most likely involves not only stereociliary changes but also alterations at the cell body level. The events taking place in these cells during and after overstimulation remain largely obscure. Cody and Russell (5) have shown that sustained depolarizations of the outer hair cells (OHCs) occur after moderately intense acoustic overstimulation and that repolarization parallels the recovery of auditory sensitivity. The underlying mechanisms are unclear.

In isolated OHCs, mechanical overstimulation results in cytoplasmic $[Ca^{2+}]$ increase (6). To investigate how this finding relates to reduced hearing sensitivity after acoustic trauma, the guinea pig isolated temporal bone preparation (7) was used to perform simultaneous investigations of calcium-dependent fluorescence, stimulus-evoked cochlear potentials and cochlear morphology. The sensory cells were visualized *in situ* in an almost native environment, and the cochlear electric responses were recorded. The preparation was used previously to study changes of organ of Corti mechanics following acoustic trauma (8) and has now been further improved, incorporating a perfusion system that enhances the preservation of mechanic and electric nonlinearities (9) as well as providing the possibility to load the sensory cells with fluorescent indicators of cell function (10).

METHODS

The procedures for dissection of the temporal bone have been described (7, 9, 10). In brief, young pigmented guinea pigs were decapitated and their temporal bones rapidly removed, opened, and immersed in Hanks' balanced salt solution with 5 mM Hepes (temperature 21–24°C). A small hole was drilled in the scala tympani of the basal turn, providing an entrance for a thin plastic tubing connected to a reservoir filled with oxygenated Hanks' solution. An opening also was made at the apex of the cochlea, through which the organ of Corti could be viewed. A 2-8-MΩ borosilicate glass microelectrode was advanced, under microscopic control, to a position where it touched Reissner's membrane, which was penetrated using a step motor. An Ag/AgCl wire in the fluid surrounding the cochlea served as the ground electrode. The average endocochlear potential (EP) was +10.2 mV (SE 3.6 mV, range −29 to +25 mV), with a positive voltage in 13 of 15 cases, zero voltage in one preparation and a negative voltage in one. The EP is strongly temperature dependent (11), and because the experiments were conducted at room temperature, the maximum value that could be recorded was lower than that found in the living animal. It has, however, been shown (12) that a decrease in temperature (to 30°C) affects neither the cochlear microphonics (CM), the summating potential, nor the auditory nerve action potential of the apical turn. The procedures for recording the electrophysiologic responses of the preparation, using a Hewlett–Packard 35665A frequency analyzer, have been described (10). Because the CM is generated primarily by

The publication costs of this article were defrayed in part by page charge payment. This article must therefore be hereby marked "*advertisement*" in accordance with 18 U.S.C. §1734 solely to indicate this fact.

Abbreviations: $[Ca^{2+}]$, calcium concentration; CM, cochlear microphonic potential; OHC, outer hair cell; CCD, charge-coupled device; dB SPL, dBre 20 μPa; EP, endocochlear potential; HeC, Hensen cells; SC, stereocilia.

†To whom reprint requests should be addressed. e-mail: anders.fridberger@fyfa.ki.se.

the OHCs (13), it was used as an index of OHC function. Because of the space constant of the scala media, the tuning of the CM will be less sharp than the tuning of the individual OHCs (14).

Sound Stimulation. The sound stimulus was provided by a Sokolich calibrated acoustic transducer (Custom Sound Systems, Newport Beach, CA). For overstimulation, a Technics HP850 loudspeaker (Matsushita Electric, Japan) was used. The overstimulation was delivered as tone bursts with 0.7 s duration, rate 1/s, at the best frequency of each particular preparation. The best frequency was defined as the frequency evoking maximum CM response. The sound pressure, measured by a probe microphone placed near the tympanic membrane, was in the range of 122–144 dB SPL in the 17 cochleas used in this study (mean 130 dB SPL). The immersion of the middle ear structures in the tissue culture medium caused a 30–35 dB reduction of the stimulus reaching the inner ear (through the fluid load on the cochlear side of the tympanic membrane; cf. 15). No attempt was made to correct for this effect in the subsequent data presentation.

Imaging of the Cochlear Structures. A custom built microscope with a Zeiss 40X, NA 0.75 lens equipped with a Hamamatsu C5985 chilled CCD camera (Hamamatsu Photonics, Hamamatsu City, Japan), was used to observe the cochlear structures. A stepping motor was connected to the microscope to allow remote control of the focal plane. Before the acquisition of a fluorescence image, an image was recorded using incident light from a fiber optic light guide positioned close to the cochlea. This light microscopic image served as a control so that the focal plane remained constant and also to provide an assessment of organ of Corti morphology. In most experiments, the image size was 734×509 pixels with a pixel size of 0.22×0.22 μm. To measure the cytoplasmic free $[Ca^{2+}]$, the Ca^{2+} sensitive dye Fluo-3/AM (Molecular Probes) was used. Dimethyl sulfoxide (Sigma) at a final concentration of 0.6–0.8% was used as a solvent together with 0.08% Pluronic F-127 (Molecular Probes), giving a dye concentration in the perfusate of 8 μM (loading time 20–30 min). Before the organ was loaded with the dye, a background image was acquired to serve as a control of the amount of autofluorescence. Epifluorescence illumination was provided by a Zeiss HBO50 mercury lamp by using a 450–490-nm bandpass filter and a 510-nm dichroic mirror for the excitation and a 520-nm long-pass filter for the emission (Zeiss). In most experiments, 10 μM of the Ca^{2+} ionophore ionomycin (Calbiochem; dissolved in 0.07% dimethyl sulfoxide) was added at the end of the experiment. Because this substance permeabilized the cell membranes selectively to Ca^{2+}, it was used to verify that the fluorescence changed in response to elevations of the intracellular $[Ca^{2+}]$.

Image Analysis. The images acquired from the CCD camera were further processed off-line using the no–neighbors algorithm (16). This algorithm removed unwanted out-of-focus information from fluorescence images, thus yielding a deblurred image. Excellent summaries of the techniques used can be found in refs. 16, 17, and 18. In brief, out-of-focus information is subtracted from the image, followed by correction for the in-focus point spread function of the lens. The contribution from out-of-focus light is estimated by convolving the image with the out-of-focus point spread function. This approach has been shown to yield results comparable with more complicated algorithms using several focal planes (e.g., ref. 17).

The point spread function of the microscope was determined using 200-nm fluorescent latex beads (Molecular Probes) in a manner similar to that described in refs. 18 and 19. The latex beads were dried onto a coverslip and covered with Hanks' solution. Images of the bead at different focal planes were taken by stepping with the focus motor, beginning several micrometers above the bead and continuing through the in-focus plane. The results obtained were very similar to those of Hiraoka *et al*. (19).

The fluorescence images acquired during the experiments had nonzero intensities near the borders of the image. To avoid high-frequency distortions caused by Fourier transformation of such images, each image was multiplied by a two-dimensional Kaiser–Bessel window (20). This procedure, however, caused the loss of information near the borders of the image and consequently, the final size of the processed image became 542 by 310 pixels.

Measurement of the fluorescence intensity of the images was performed using the METAMORPH image analysis package (v 2.75; Universal Imaging, West Chester, PA). Regions of interest corresponding to the cell bodies of two or three OHCs were defined in the processed images, and the average intensity of each region was measured on all images from a given experiment. The average fluorescence intensity of the whole unprocessed image also was measured, giving results qualitatively similar to the measurements on the processed images. The percentage change in fluorescence shown in the subsequent graphs was calculated by means of the formula:

$$\% = [(F - F_b)/(F_{initial} - F_b)]^*100,$$

where F is the average fluorescence intensity of the region of interest, F_b is the intensity of the background image, and $F_{initial}$ is the fluorescence intensity of the first fluorescence image of each experiment.

Confocal Microscopy. To ascertain that the deblurred images were representative, the organ of Corti also was visualized using a Biorad MRC 1024 laser scanning confocal microscope. The procedures for the dissection and loading of the organ were identical with those used in the other parts of this study, but the cochlear potentials were not recorded. The confocal microscope produced images very similar to the deblurred images (e.g., Fig. 1), and the cellular distribution of the dye appeared identical.

RESULTS

Figure 1*A* shows a cross-section of the organ of Corti drawn from light and electron microscopic images of the apical turn of the guinea pig's cochlea. In the apical turn, the three rows of OHCs (dark gray) are at an angle of $\approx 30°$ with respect to the basilar membrane (BM). Thus, a 30° tilting of the preparation allows the OHCs to be viewed along their long axis, as indicated by the optical plane illustrated in the drawing. Fig. 1*B* shows an image acquired by the confocal microscope at this focal plane, after loading the organ with Fluo-3. The dye had a cytoplasmic distribution, and the cell bodies of several OHCs can be clearly seen with the hair bundle region facing the left side of the image. The characteristic lipid droplets of the Hensen cells (HeC) are out of focus. Fig. 1*C* shows a fluorescence image acquired from another preparation loaded with Fluo-3. This image has low contrasts, and the outlines of the sensory cells can be barely perceived. After processing with the no–neighbors algorithm, the resolution improved and the cell bodies of several OHCs now can easily be identified (Fig. 1*D*). The similarity to the image acquired with the confocal microscope (Fig. 1*B*) is apparent. The no–neighbors algorithm was chosen because it permits images to be collected rapidly under low light conditions, which reduces bleaching of the indicators and laser-induced phototoxic damage to the preparation.

Changes of Intracellular Ca^{2+} Levels After Acoustic Overstimulation. Fig. 2 shows a typical example of processed fluorescence images, with the hair bundle region facing the left part of the image and the nuclear pole of the cells to the right. Fig. 2*A* shows a group of OHCs before overstimulation, and Fig. 2*B* shows the same hair cells after exposure to a 153 Hz repeated tone at 131 dB SPL, duration 15 min The outlines of

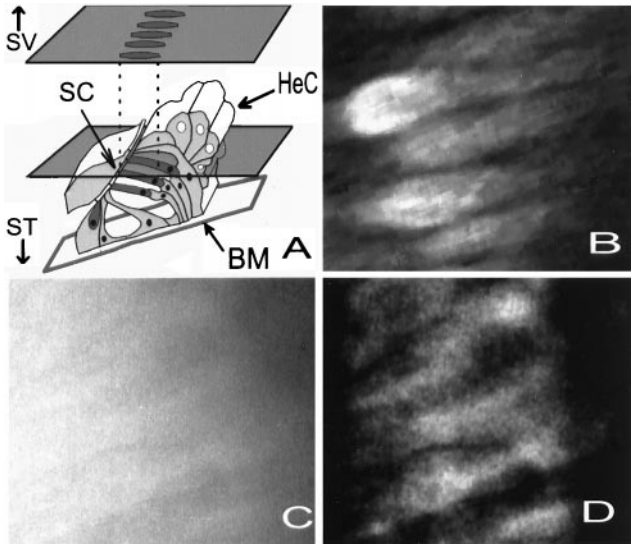

FIG. 1. (*A*) Schematic drawing of the organ of Corti in the apical turn of the guinea pig cochlea, made from light and electron microscopic images. The plane of section through the organ seen in *B–D* is indicated by the plane through the figure. By tilting the preparation, the cell bodies of the OHCs were visualized. During the experiments, the organ was viewed from the scala vestibuli (SV) side. ST, direction of the scala vestibuli; BM, basilar membrane. Hair cells dark gray. (*B*) Confocal microscope image. (*C*) Fluorescence image. See text for explanations. (*D*) Fig. 1*C* after processing with the no–neighbors algorithm.

three different OHCs also have been included in the images. The exposure caused a 28% increase in the Ca^{2+} signal.

Fig. 3 shows data from a preparation that was subjected to a tone at 127 dB SPL for 15 min with the frequency set to the best frequency of the preparation (153 Hz). The overstimulation period is marked by the vertical bar in Fig. 3*A* showing the amplitude of the CM at a stimulus level of 84 dB SPL. A 2-dB increase of the CM was seen during the 20 min that preceded the exposure, and the overstimulation resulted in a 19-dB reduction. No sign of recovery of the CM was seen after the termination of the stimulus, but rather the amplitude continued to decrease for the remaining 49 min of the experiment. The fluorescence intensities of three different OHCs also was measured (Fig. 3*B*), each point in the graph representing the average fluorescence of these three cells. Four images showing a stable Ca^{2+} signal were acquired during 18 min before the overstimulation, and the overstimulation resulted in a 60% increase in the average fluorescence. There was no sign of recovery of the elevated Ca^{2+} levels in this experiment, but rather the $[Ca^{2+}]$ remained elevated for the duration of the experiment.

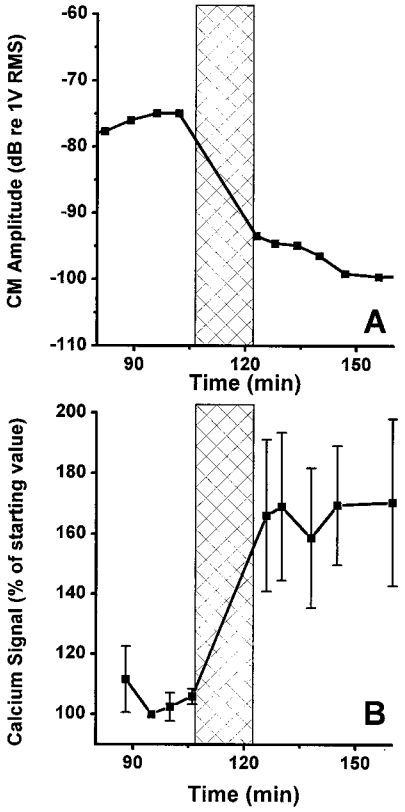

FIG. 3. (*A*) Recording of the CM amplitude before and after acoustic overstimulation. The overstimulation period is indicated by the crossed region. (*B*) Ca^{2+}-dependent fluorescence in the same preparation as shown in *A*. Vertical bars centered on each point give the SE. The overstimulation resulted in a 60% increase of the fluorescence.

A different pattern was seen in the experiment shown in Fig. 4. In this experiment, the CM was measured at a stimulus level of 77 dB SPL. The best frequency of the preparation was 137 Hz, and the CM was stable to within 2.5 dB before the overstimulation. Immediately after 15 min of acoustic overstimulation at 125 dB SPL (137 Hz), the amplitude had decreased by 13 dB (Fig. 4*A*). This initial decrease was, however, rapidly recovered and the CM had completely returned to the initial level 21 min after the cessation of the stimulus. The overstimulation produced an 85% increase in the Ca^{2+} signal (Fig. 4*B*), with the peak values recorded immediately after the cessation of overstimulation. A tendency towards recovery of the elevated Ca^{2+} levels was seen, and 30 min after the end of the stimulation, the fluorescence was 70% above the prestimulus level.

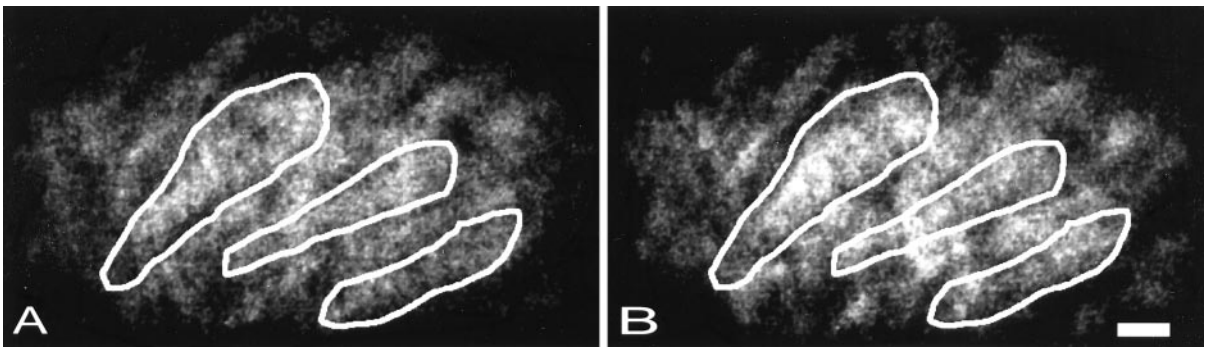

FIG. 2. (*A*) A group of OHCs in the apical turn loaded with Fluo-3. (*B*) the same group of cells after being subjected to acoustic overstimulation. (Scale bar: 10 μm.)

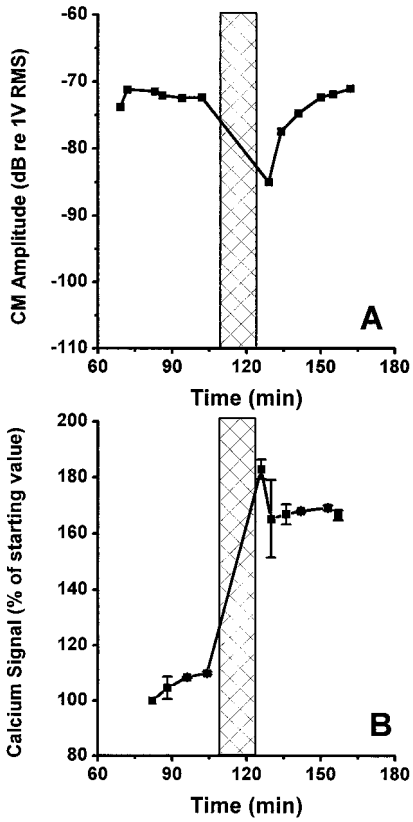

FIG. 4. (*A*) Overstimulation resulted in a transient decrease of the amplitude of the CM in this preparation, but the amplitude returned to the prestimulus level in 21 min after ending the stimulus. (*B*) Fluorescence measurement from the same preparation. After the termination of the stimulus period, partial recovery was seen.

Ca^{2+} increases such as the ones shown above were seen in 12 of 14 preparations. The mean increase was 44% (SE 7%) which was measured immediately after the termination of the overstimulation. Twenty minutes later, the average fluorescence in these 14 preparations was 60% (SE 8%) above the baseline, illustrating that a continuous Ca^{2+} increase occurred in many preparations after ending the stimulus. In two preparations, partial recovery was noticed, and one preparation showed an almost complete recovery. These preparations were stimulated at levels in the lower range of those used in this study, and the CM recovery pattern was similar to that of Fig. 4. Thus, in some preparations, the OHCs retained the ability to regulate the cytoplasmic $[Ca^{2+}]$ even after acoustic overstimulation.

Several experiments also were performed at lower stimulus levels, between 110 and 120 dB SPL for 10 or 15 min These exposure intensities were not sufficient to provoke a change of the CM amplitude with the exposure durations used in this study. In these experiments, Ca^{2+} increases were not seen (data not shown). Also, it is evident from the experiments shown in Figs. 3, 4, and 6 that stimulation at normal intensities (between 75 and 88 dB SPL) does not produce detectable Ca^{2+} increments.

As can be seen in the present data, there does not appear to be a straightforward relationship between the $[Ca^{2+}]$ and the amplitude of the CM. The acoustic trauma caused an increase in the $[Ca^{2+}]$ and a decrease in the CM, but after ending the stimulus, the CM does not appear to be related to the $[Ca^{2+}]$. In several experiments, clear recovery of the CM was seen in spite of continuous high Ca^{2+} levels. However, in the preparations showing recovery of the $[Ca^{2+}]$ changes, the CM also showed substantial recovery. Because these preparations were stimulated at slightly lower levels, it is possible that the $[Ca^{2+}]$ and the CM are linked at these levels.

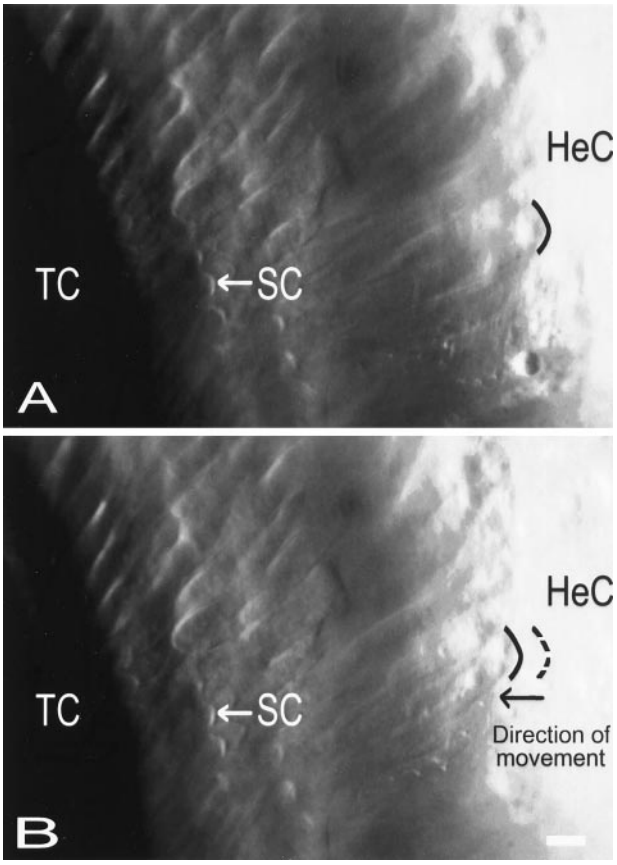

FIG. 5. Photomicrographs showing the surface of the organ of Corti in the apical turn. The HeC can be seen in the *Right* part of the image; the characteristic lipid droplets inside their cytoplasm being evident as the round structures. The tunnel of Corti (TC) is to the left, and immediately to the right of the tunnel, the first row of OHCs is seen. The arrows indicate the location of the characteristically V-shaped hair bundle (SC) of a second row outer hair cell. (*A*) Before overstimulation. (*B*) After overstimulation. The result of the stimulus was a contraction of the organ. The position of the SC remained constant, but the HeC moved in the direction of the tunnel of Corti. The contraction was associated with a 10 dB decrease of the CM and an increase of the $[Ca^{2+}]$. (Bar = 10 μm.)

Previous studies (21, 22), using either ionophores or alterations in perilymphatic Ca^{2+} to change the hair cell Ca^{2+} levels, have not showed any relationship between the Ca^{2+} level and the amplitude of the CM. Nonetheless, the Ca^{2+} ionophore ionomycin was used at concentrations of either 2.5 or 10 μM to increase the organ of Corti $[Ca^{2+}]$, to clarify the relation between the Ca^{2+} changes and the CM. The high concentration produced much larger increases of the Ca^{2+} levels than did the noise trauma, but regardless of this increase, there was no change in the CM. In a few experiments, an increase in the CM was observed when the Ca^{2+} levels were elevated, but this increase was paralleled by an increase in the EP. The low ionophore concentration caused smaller alterations of the $[Ca^{2+}]$ without effects on the CM.

Organ of Corti Contraction. The light microscopic images that were acquired before the fluorescence images permitted the assessment of organ of Corti morphology before and after the acoustic trauma. Interestingly, it was found that large amplitudes of acoustic stimulation altered the structure of the hearing organ in a very specific way. After overstimulation, the width of the hearing organ, measured as the distance between the outer edge of the HeC and the outer hair cell stereocilia (SC), decreased. For clarity, these structures also have been

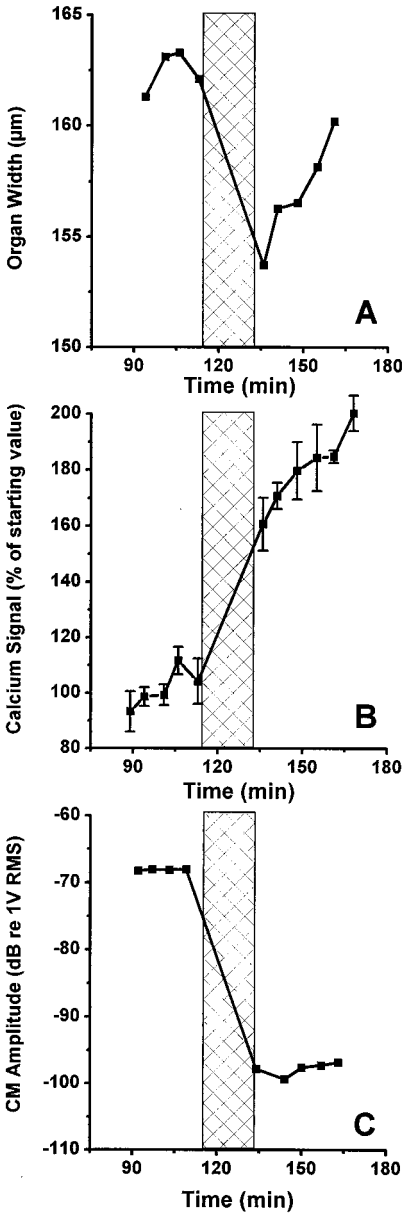

FIG. 6. (*A*) Measurement of the width of the hearing organ before and after overstimulation. A large contraction followed the noxious stimuli, with full recovery occurring in the subsequent 25 min (*B*) Ca^{2+}-dependent fluorescence from the same preparation. (*C*) Measurement of the CM amplitude in response to an 88-dB SPL stimulus before and after overstimulation.

included in the cross-section shown in Fig. 1*A*. In most cases, partial or complete recovery occurred during 30–45 min after ending the traumatizing stimulus. Fig. 5 shows an example of typical changes occurring as a consequence of acoustic trauma. Before the overstimulation (Fig. 5*A*), the distance between the OHC SC and the HeC was 84 μm. The SC retained their position after 15 min of overstimulation at 129 dB and 153 Hz, but the HeC moved 6 μm in the direction of the tunnel of Corti (TC). To clarify this, the black curved line marks the position of the inner border of the HeC. After overstimulation (Fig. 5*B*), this cellular structure moved closer to the tunnel of Corti, the dashed line indicating the position before the overstimulation. Structural changes such as these occurred in 10 of 14 preparations. The remaining preparations showed either no change or contractions or elongations that appeared unrelated to the acoustic trauma. The average change of the organ of Corti width was 9 μm (SE 2 μm) in the 10 preparations.

Fig. 6 gives data from another preparation, highlighting the dynamic nature of the structural changes. Before the acoustic trauma, the distance between the first row of OHCs and the outer edge of the HeC was 160 μm (Fig. 6*A*). Overstimulation at 129 dB induced a contraction of the organ, the distance decreasing to 154 μm. In the 25 min after ending the overexposure stimulus, the hearing organ returned close to its original width. Fig. 6*B* shows the measured fluorescence from the same preparation. A large increase in $[Ca^{2+}]$ occurred as a consequence of the trauma. After the exposure, the Ca^{2+} signal continued to increase without showing any sign of reversibility. The trauma also brought about a 29-dB decrease in the CM (Fig. 6*C*).

DISCUSSION

The findings of the present study can be summarized as follows: (*i*) Acoustic overstimulation causing diminished CM amplitude also caused sustained increases in the $[Ca^{2+}]$ of the OHCs. The Ca^{2+} changes followed immediately after the acoustic trauma, and partial recovery of the elevated levels were seen in some cases. (*ii*) Acoustic overstimulation also led to a decrease in the width of the hearing organ. This contraction was often reversible, and a nearly complete recovery was seen in several cases. The contraction appeared to be an acute response to the acoustic trauma that often subsided in 30–45 min

What Is the Role of Ca^{2+} in the Pathogenesis of Acoustic Trauma? The Ca^{2+} increases that were seen in the present study had slow kinetics. It is well established that a sustained increase in intracellular $[Ca^{2+}]$ is toxic to cells (reviewed in refs. 23 and 24) through activation of numerous calcium-dependent enzymes. After elevations of Ca^{2+}, the actin cytoskeleton is rearranged through the activation of proteinases (25). This process may result in rounding of the cells or the formation of cytoplasmic blebs. These effects have been shown in a variety of cell types after toxic injury and can be blocked if the Ca^{2+} increase is prevented (26). In the present study, both changes in cell shape and the formation of blebs could be occasionally seen after noise exposure. $[Ca^{2+}]$ increases also have been reported to activate endonucleases, which fragment the DNA (24, 27), causing the induction of apoptosis. Recently, it also has been shown that a sustained increase in intracellular $[Ca^{2+}]$ of the hair cell blocks the regeneration of the tip links connecting the SC (28). After overstimulation, these mechanisms may impair the recovery of hearing sensitivity or cause degeneration of the hair cells.

What Is the Source of the Ca^{2+}? It has been shown that Ca^{2+} ions enter through the transducer channels of vertebrate hair cells during maintained deflections of the hair bundle (29, 30, 31). Ikeda *et al*. (32) found that acoustic trauma caused a 50-fold increase of the $[Ca^{2+}]$ in the endolymph, thus generating an increased concentration gradient. Consequently, increased entry through the transducer channels followed by exhaustion of the cell's Ca^{2+} regulating machinery may be one explanation for the Ca^{2+} changes observed in the present study.

Following overstimulation, the stereocilia may be damaged (2), making the transducer channels a less likely path for Ca^{2+} entry. In this situation, Ca^{2+} entry through the basolateral membrane of the OHCs also is possible because voltage-activated Ca^{2+} channels are present in hair cells (reviewed in ref. 33). It is also possible that acoustic trauma causes damage to cellular organelles, leading to Ca^{2+} release from intracellular stores.

Contraction of the Hearing Organ. Noise-induced contractions of the organ of Corti have been noticed before (8, 34, 35, 36), although the dynamic nature of the changes has not been appreciated. This fact is not surprising, since most studies dealing with the morphologic consequences of noise trauma

have employed histologic techniques, providing a ''snapshot'' of a highly dynamic process. To the best of our knowledge, the present study is the first to demonstrate the dynamic nature of noise-induced structural alterations. Because these structural changes were fully reversible in several cases, it is unlikely that they represent a collapse (36) of the supporting elements of the organ. Rather, it seems to be an active response of the auditory periphery to acoustic injury.

Several cell types in the organ of Corti have the capacity to actively change their length. The most well-documented is the slow motility of the OHC (37), but motility of isolated Deiters' cells also has been described (38). In some cases (*e.g.*, Fig. 6), reversal of the contraction was seen in spite of continuous high Ca^{2+} levels. This result does not rule out Ca^{2+} as an important regulator of the contraction response. For instance, in smooth muscle cells, contraction is initiated by Ca^{2+}-induced phosphorylation of the myosin light chains. The force is dependent on the phosphorylation, and consequently, the force may decline in spite of continuous high Ca^{2+} levels (*e.g.*, ref. 40). A similar mechanism is possible in the hearing organ. The OHCs also show a Ca^{2+}-dependent decrease of cellular stiffness (39), and, due to their pivotal position in the hearing organ, a stiffness change could both alter the micromechanic behavior of the organ and promote the type of morphologic changes described here. Normal cochlear transduction is dependent on the spatial relationships between the hair cells, the basilar membrane and the tectorial membrane (41, 42, 43). Thus, regardless of the cellular origin(s) of the contraction response, it will have profound effects on the performance of the organ.

The mechanisms behind the process of repair leading to the recovery of hearing sensitivity after trauma are essentially unknown. The finding of elevated hair cell Ca^{2+} levels after overstimulation has important implications, given the ubiquitous role of Ca^{2+} as a second messenger and the presence of Ca^{2+} regulatory proteins throughout the hair cell cytoplasm (44). Today, the possibilities for enhancing the recovery of hearing sensitivity after noise damage are very limited. Blocking the entry of Ca^{2+} ions might provide a means of restricting the harmful effects of noise on the auditory periphery.

We thank Drs. T. J. Keating and R. J. Cork, Purdue University, for the generous gift of the C source code of the deconvolution software. Dr. J. T. P. W. van Maarseveen is acknowledged for helpful discussions on digital signal processing and Dr. Joseph Bruton and Mr. O. Flock for helpful comments on the manuscript. Supported by the Swedish Medical Research Council, Stiftelsen Tysta Skolan, Hörselskadades Riksförbund, Rådet för Arbetslivsforskning, Stiftelsen Lars Hiertas minne, and Knut och Alice Wallenbergs stiftelse.

1. Saunders, J. C., Cohen, Y. E. & Szymko, Y. M. (1991) *J. Acoust. Soc. Am.* **90,** 136–146.
2. Liberman, M. C. & Dodds, L. W. (1984) *Hear. Res.* **16,** 55–74.
3. Tilney, L. G., Saunders, J. C., Egelman, E. & DeRosier, D. J. (1982) *Hear. Res.* **7,** 181–197.
4. Hamernik, R. P., Patterson, J. H., Turrentine, G. A. & Ahroon, W. A. (1989) *Hear. Res.* **38,** 199–212.
5. Cody, A. R. & Russell, I. J. (1985) *Nature (London)* **315,** 662–665.
6. Fridberger, A. & Ulfendahl, M. (1996) *Acta Oto-Laryngol.* **116,** 17–24.
7. Ulfendahl, M., Flock, Å & Khanna, S. M. (1989) *Hear. Res.* **40,** 55–64.
8. Ulfendahl, M., Khanna, S. M. & Löfstrand, P. (1993) *Eur. J. Neurosci.* **5,** 713–723.
9. Ulfendahl, M., Khanna, S. M., Fridberger, A., Flock, Å. & Jäger, W. (1996) *J. Neurophysiol.* **76,** 3850–3862.
10. Flock, Å, Flock, B., Fridberger, A. & Jäger, W. (1997) *Hear. Res.* **106,** 29–38.
11. Brundin, L., Flock, B. & Flock, Å. (1992) *Hear. Res.* **58,** 175–184.
12. Ohlemiller, K. K. & Siegel, J. H. (1992) *Hear. Res.* **63,** 79–89.
13. Dallos, P. & Cheatham, M. A. (1976) *J. Acoust. Soc. Am.* **60,** 510–512.
14. Kletsky, E. J. & Zwislocki, J. J. (1980) *Hear. Res.* **2,** 549–557.
15. Brundin, L. (1991) Ph.D. thesis (Karolinska Institutet, Stockholm, Sweden).
16. Monck, J. R., Oberhauser, A. F., Keating, T. J. & Fernandez, J. M. (1992) *J. Cell Biol.* **116,** 745–759.
17. Agard, D. A. (1984) *Ann. Rev. Biophys. Bioeng.* **13,** 191–219.
18. Keating, T. J. & Cork, R. J. (1994) *Methods Cell Biol.* **40,** 221–241.
19. Hiraoka, Y., Sedat, J. W. & Agard, D. A. (1990) *Biophys. J.* **57,** 325–333.
20. Harris, F. J. (1978) *Proc. IEEE* **66**(1), 51–83.
21. Bobbin, R. P., Fallon, M. & Kujawa, S. G. (1991) *Hear. Res.* **56,** 101–110.
22. Kössl, M., Richardson, G. P. & Russell, I. J. (1990) *Hear. Res.* **44,** 217–230.
23. Trump, B. F. & Berezesky, I. K. (1992) *Curr. Opin. Cell Biol.* **4,** 227–232.
24. Orrenius, S., McCabe, M. J. & Nicotera, P. (1992) *Toxicol. Lett.* **64/65,** 357–364.
25. Elliget, K. A., Phelps, P. C. & Trump, B. F. (1991) *Cell Biol. Toxicol.* **7,** 263–280.
26. Gilbert, R. J., Pothoulakis, C., LaMont, J. T. & Yakubovich, M. (1995) *Am. J. Physiol.* **268,** G487–G495.
27. Wyllie, A. H. (1980) *Nature (London)* **284,** 555–556.
28. Zhao, Y., Yamoah, E. N. & Gillespie, P. G. (1996) *Proc. Natl. Acad. Sci. USA* **94,** 15469–15474.
29. Ohmori, H. (1988) *J. Physiol. (London)* **399,** 115–137.
30. Denk, W., Holt, J. R., Shepherd, G. M. G. & Corey, D. P. (1995) *Neuron* **15,** 1311–1321.
31. Lumpkin, E. A. & Hudspeth, A. J. (1995) *Proc. Natl. Acad. Sci. USA* **92,** 10297–301.
32. Ikeda, K., Kusakari, J. & Takasaka, T. (1988) *Hear. Res.* **32,** 103–110.
33. Kros, C. J. (1996) in *The Cochlea*, eds. Dallos, P., Popper, A. N. & Fay, R. R. (Springer, Heidelberg), pp. 318–385.
34. Fredelius, L., Rask-Andersen, H., Johansson, B., Urquiza, R., Bagger-Sjöbäck, D. & Wersäll, J. (1988) *Acta Otolaryngol.* **106,** 81–93.
35. Dew, L. A., Owen, R. G. & Mulroy, M. J. (1993) *Hear. Res.* **66,** 99–107.
36. Harding, G. W., Baggot, P. J. & Bohne, B. A. (1992) *Hear. Res.* **63,** 26–36.
37. Flock, Å., Flock, B. & Ulfendahl, M. (1986) *Arch. Oto-Rhino-Laryngol.* **243,** 83–90.
38. Dulon, D., Blanchet, C. & Laffon, E. (1994) *Biochem. Biophys. Res. Commun.* **201,** 1263–1269.
39. Dallos, P., He, D. Z., Lin, X., Sziklai, I., Mehta, S. & Evans, B. N. (1997) *J. Neurosci.* **17,** 2212–2226.
40. Himpens, B., Matthijs, G. & Somlyo, A. P. (1989) *J. Physiol. (London)* **413,** 489–503.
41. von Békésy, G. (1960) *Experiments in Hearing*, ed. Wever, E. G. (McGraw–Hill, New York).
42. Ulfendahl, M., Khanna, S. M. & Heneghan, C. (1995) *NeuroReport* **6,** 1157–60.
43. Zwislocki, J. J. (1986) *Hear. Res.* **22,** 155–169.
44. Slepecky, N. B. & Ulfendahl, M. (1993) *Hear. Res.* **70,** 73–84.